Journal of
Synchrotron
Radiation

ISSN 0909-0495

Received 25 February 2004
Accepted 3 November 2004

Determination of the metal ordering in meteoritic $(Fe,Ni)_3P$ crystals

O. Moretzki,[a] W. Morgenroth,[b] R. Skála,[c] A. Szymanski,[a] M. Wendschuh[d] and V. Geist[a]*

[a]Institut für Mineralogie, Kristallographie und Materialwissenschaft der Universität Leipzig, Scharnhorststrasse 20, 04275 Leipzig, Germany, [b]Mineralogisch-Petrologisches Institut und Museum der Universität Bonn, Poppelsdorfer Schloss, D-53115 Bonn, Germany, [c]Czech Geological Survey, Prague, Czech Republic, and [d]Zentrallabor für Kristallographie und angewandte Materialwissenschaft (ZEKAM), Universität Bremen, Klagenfurter Strasse, D-28359 Bremen, Germany. E-mail: geist@rz.uni-leipzig.de

Synchrotron radiation diffraction studies of meteoritic $(Fe,Ni)_3P$ crystals have been performed to reveal the ordering of the elements Fe and Ni on the three metal sites M1, M2 and M3 of the unit cell. The δ synthesis technique, which is a two-wavelength method using anomalous dispersion effects, was applied. For (Fe,Ni) phosphide crystals with different Fe:Ni ratios extracted from different meteorites, it was found that Ni occupies the M3 site and also partially the M2 site, avoiding the M1 position, whereas the M1 site is preferentially occupied by Fe. In connection with earlier results known from the literature, this metal distribution seems to be characteristic of this compound, and is independent of thermodynamic formation conditions.

Keywords: meteorites; schreibersite; rhabdite; metal order; δ synthesis; anomalous scattering.

1. Introduction

The main phases in iron meteorites comprise of kamacite (α-Fe,Ni, b.c.c.) and taenite (γ-Fe,Ni, f.c.c.). Next to them, several minor phases occur in meteoritic irons including mainly troilite (FeS), cohenite (Fe_3C) and schreibersite [$(Fe,Ni)_3P$] (Buchwald, 1975).

The phosphides of composition $(Fe,Ni)_3P$ appear in different morphological forms. Traditionally, the term schreibersite describes macroscopic inclusions, lamellae and precipitates, whereas the term rhabdite, representing a variety name, is restricted to prismatic idiomorphic crystals. The differences in the morphology are interpreted as a result of heterogeneous and homogeneous nucleation mechanisms. Fe_3P and Ni_3P show complete mutual solubility; the concentration of Ni in meteoritic $(Fe_{3-x}Ni_x)P$ phosphides ranges between 7 and 65 wt% (Doan & Goldstein, 1970; Reed, 1965; Clarke & Goldstein, 1978). The crystal structure of a meteoritic $(Fe,Ni)_3P$ crystal (rhabdite from the North Chile iron meteorite with Fe:Ni $\simeq$ 2:1) was first determined by Doenitz (1970): it crystallizes in the tetragonal space group $I\bar{4}$ (#82) with cell dimensions a = 9.040 Å and c = 4.462 Å, containing eight formula units per unit cell. The synthetic Fe_3P and Ni_3P show the same structure (Aronsson, 1955; Rundquist, 1962).

In this structure, three crystallographically non-equal metal sites M1, M2 and M3 exist (Fig. 1). In the case of $(Fe_{3-x}Ni_x)P$ the question concerning the distribution of the two elements Fe and Ni over these positions arises. Fe and Ni are either distributed homogeneously or with a preferred site occupancy (ordering). The existence of both isotype binary compounds, Fe_3P and Ni_3P, indicates that Fe and Ni are able to occupy each metal site in general. Therefore, the structure itself gives no hints concerning the type of distribution. Using conventional

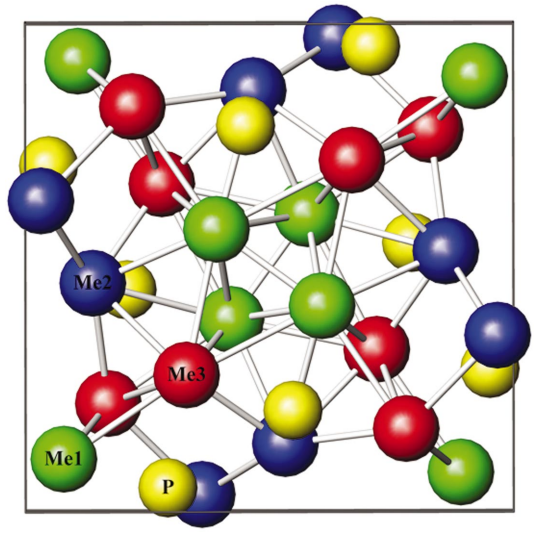

Figure 1
The $(Fe,Ni)_3P$ structure projected onto the (001) plane.

X-ray diffraction methods, a precise differentiation between Fe and Ni on different structural sites is difficult because of their close scattering power. Hence, Doenitz (1970) determined the Fe:Ni distribution using the anomalous scattering of Co $K\alpha$ radiation. Concerning the rhabdite crystal mentioned above, it was shown by Doenitz that Ni occupies the metal sites M3 and M2, avoiding M1 (M1: Fe; M2: $\frac{2}{3}$Fe + $\frac{1}{3}$Ni; M3: $\frac{1}{3}$Fe + $\frac{2}{3}$Ni).

It was proposed (*e.g.* Skála & Císařová, 2001*a*) that the metal distribution of the meteoritic phosphides may be related to the thermal history of the meteorites. A number of structure determinations on $(Fe,Ni)_3P$, mainly using Mo $K\alpha$ radiation, were performed to estimate the metal distribution (Skála & Drábek, 2003, and references therein; Skála & Císařová, 2001*a*,*b*; Jörchel *et al.*, 2000; Moretzki *et al.*, 2003). The results were predominantly in agreement with those of Doenitz (1970). Thus the question arose as to whether this distribution is a general feature found in $(Fe,Ni)_3P$ or whether it reflects some special conditions ruling during the crystallization.

An elegant method for differentiating elements with similar scattering power in different structural sites is the so-called δ synthesis, which is a two-wavelength method using anomalous dispersion effects (Wulf, 1990; Wendschuh-Josties, 1990, 1994; Moretzki, 1999). The application of synchrotron radiation is indispensable here, owing to the need for a free choice of wavelengths and a high-intensity beam; the latter is important for experiments with small samples as the meteoritic phosphide crystals.

In general, synchrotron radiation has been applied in the study of iron meteorites including trace-element analysis (*e.g.* Sutton *et al.*, 1987), determination of the oxidation state of Fe by XANES (Delaney & Dyar, 2003), investigations of superstructure in taenite (*e.g.* Tagai *et al.*, 1992) and of the orientation relation between kamacite and taenite (Bunge *et al.*, 2003).

The δ method requires the recording of two data sets with different wavelengths selected near the absorption edge of one of the elements in demand, favourably the lighter ones. Between the two used wavelengths a gradient in the dispersion factor f' should exist, and the absorption ($\sim f''$) should be unchanged. In this way the difference in the two data sets reflects only the actual value of f'. The location of atoms within the unit cell must be known *a priori* and only the site occupancy of the metals can be determined. The phases of the structure factors have to be calculated using a preliminary model of the element distribution (*e.g.* a statistical model). Then the calculated phases φ_C are assigned to the measured moduli $|F_O|$. As a result, a partly calculated, partly measured ('mixed') structure factor F_{mh} is obtained. The factor D_{mh}, called the delta coefficient, is then yielded as the difference of both structure factors according to

$$D_{mh} = F_{mh}(\lambda_1) - F_{mh}(\lambda_2).$$

With a set of such D_{mh} factors as coefficients, the difference electron density,

$$\rho_D(x) = \sum_h D_{mh} \exp(2\pi i h x),$$

can be calculated. This difference electron density shows maxima only in the positions of atoms with a certain change in scattering power. In order to avoid confusion with the conventional $F_O - F_C$ difference syntheses, the described difference is called δ synthesis.

It should be noted that δ synthesis is a robust method because specific errors are eliminated by the difference procedure. It is important, however, that a reflection (*hkl*) at both wavelengths has almost the same integral intensity.

This technique was successfully applied to centrosymmetrical crystals like galenobismutite, spinel and perowskite, but only to one acentric crystal (mückeite). For the chalcopyrite structure, which is also an acentric structure, it was shown that the δ method was not suitable (Wendschuh-Josties, 1990). Because the structure of $(Fe,Ni)_3P$ is acentric, the question of how far the δ method is applicable for the investigation of meteoritic phosphides was still open.

2. Experimental

2.1. Samples

Figs. 2(*a*) and 2(*b*) show rhabdite and schreibersite crystals embedded in the meteorites. In this form the crystals can be characterized by electron microprobe, optical methods, electron back-scattered diffraction (EBSD) and other techniques. The contents of Fe and Ni in a rhabdite crystal, determined by electron microprobe line-scan, is given in Fig. 3. The single-crystal samples used in the X-ray diffraction experiments were extracted by a chemical treatment of the meteorite region of interest (*cf.* Jochum *et al.*, 1980).

Phosphides from the following meteorites were investigated: Toluca (IAB), Canyon Diablo (IAB), Odessa (IAB), Sikhote Alin (IIAB), Orange River (IIAB), Morasko (IIICD), Carlton (IIICD) and Watson (IIE). All these meteorites are octahedrites with different bandwidths of the kamacite lamellae. Also the chemical classification of the iron meteorites (IAB, IIAB, IIIAB, IIICD and IIE) is given.

The brittle phosphides are often broken owing to the plastic deformation of the ductile Fe/Ni matrix. Because the schreibersite crystals are mostly relatively large, it is possible to find parts with good crystalline quality, whereas the small rhabdite crystals cannot be divided further. Table 1 shows the structural data of the phosphides determined by conventional X-ray methods as a preliminary investigation to the synchrotron experiments.

It should be noted that it was not possible to obtain suitable rhabdite crystals from all meteorites investigated. A correlation of the phosphide quality to the varying history of the corresponding meteorite could be possible (see also Geist *et al.*, 2005).

In the unit cell, the atoms are arranged in four layers aligned perpendicular to the *c* axis and ordered approximately at 0, 0.25, 0.5 and 0.75. Each layer is composed of eight atoms (Table 2).

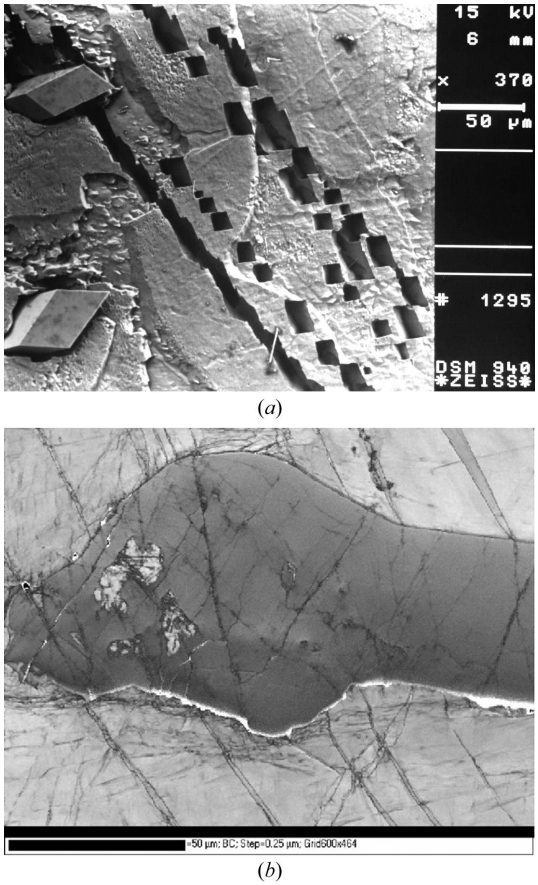

Figure 2
Examples of the two different forms of meteoritic phosphides. (*a*) A scanning electron microscopy image of etched rhabdite crystals in kamacite (Toluca meteorite). (*b*) An EBSD pattern (band contrast mode) of a schreibersite crystal in kamacite (Watson meteorite). A number of fine microcracks, which are arranged parallel to the crystallographic planes, are visible in the schreibersite. The microcracks can be interpreted as an indicator of brittle fracture, whereas the kamacite shows the known twinning planes as a result of the plastic deformation.

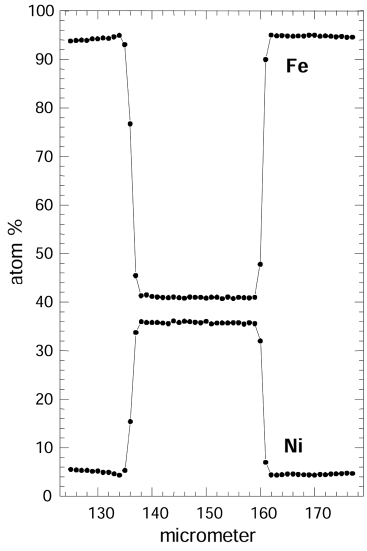

Figure 3
Contents of Ni and Fe in a rhabdite crystal embedded in kamacite (Toluca). The diameter of the crystal was about 30 µm.

Table 1
Structural data of selected phosphides obtained with a four-circle X-ray diffractometer/imaging-plate diffraction system and a microprobe.

The schreibersite samples are from the Czech Geological Survey, Prague.

Rhabdite (Toluca) [a = 9.0240 (6) Å, c = 4.4670 (4) Å, Fe:Ni $\simeq$ 1.2:1]				
	x	y	z	U_{iso}
M1	0.0779 (1)	0.1081 (1)	0.2292 (2)	0.010 (1)
M2	0.3621 (1)	0.0339 (1)	0.9794 (2)	0.006 (1)
M3	0.1678 (1)	0.2189 (1)	0.7482 (2)	0.010 (1)
P	0.2928 (2)	0.0507 (2)	0.4832 (5)	0.009 (1)

Schreibersite (Odessa) [a = 9.0810 (5) Å, c = 4.4631 (6) Å, Fe:Ni $\simeq$ 1.5:1]				
	x	y	z	U_{iso}
M1	0.0794 (1)	0.1071 (1)	0.2278 (2)	0.010 (1)
M2	0.3616 (1)	0.0322 (2)	0.9812 (2)	0.005 (1)
M3	0.1703 (1)	0.2191 (1)	0.7489 (2)	0.011 (1)
P	0.2917 (2)	0.0474 (2)	0.4861 (5)	0.009 (1)

Schreibersite (Sikhote Alin) [a = 9.0753 (3) Å, c = 4.4722 (5) Å, Fe:Ni $\simeq$ 2:1]				
	x	y	z	U_{iso}
M1	0.0792 (2)	0.1069 (2)	0.2294 (3)	0.009 (1)
M2	0.3604 (3)	0.0323 (3)	0.9821 (3)	0.008 (1)
M3	0.1706 (2)	0.2194 (2)	0.7517 (2)	0.010 (1)
P	0.2908 (4)	0.0467 (4)	0.4873 (8)	0.007 (1)

Table 2
Arrangement of crystal atoms along the z direction shown for the schreibersite crystal of the iron Sikhote Alin (*cf.* Table 1).

All sites appear twice.

z	Site
0.987	P
0.982	M2
0.771	M1
0.752	M3
0.748	M3
0.729	M1
0.518	M2
0.513	P
0.487	P
0.482	M2
0.271	M1
0.252	M3
0.248	M3
0.229	M1
0.018	M2
0.013	P

2.2. Data collection

The experimental method of the δ synthesis as described above was performed at beamline D3 (four-circle diffractometer) at the synchrotron facility HASYLAB at DESY, Hamburg, Germany. A suitable wavelength region for the application of the δ method is the low-energy side of the Fe edge (see Fig. 4) because the variation of the absorption of Fe and Ni is small. Otherwise f'_{Fe} shows strong and f'_{Ni} only less variation. The first wavelength λ_1 has to be chosen as close as

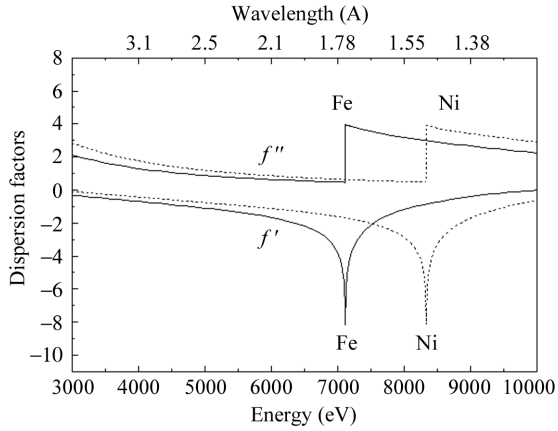

Figure 4
The dispersion terms f' and f'' for Fe and Ni (http://www-phys.llnl.gov/Research/scattering/index.html).

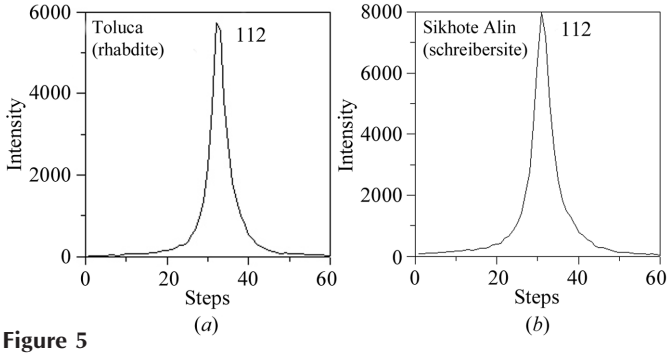

Figure 5
(*a*) 112 reflection profile of a schreibersite crystal from the Sikhote Alin meteorite (stepwidth $\Delta\omega = 0.006^\circ$). (*b*) 112 reflection profile of a rhabdite crystal from the Toluca meteorite (stepwidth $\Delta\omega = 0.003^\circ$).

possible to the absorption edge of Fe to obtain the largest possible difference in $f'_{\rm Fe}$. The choice of the second wavelength λ_2 is not so critical and it was selected on the slowly increasing part of $f'_{\rm Fe}(E)$.

After testing the phosphide crystals (as examples the 112 reflection profiles measured are shown in Fig. 5), data sets near the Fe edge were recorded. The position of the Fe absorption edge was determined by measuring the (411) reflection intensity at energies between 7000 and 7250 eV in steps of 2 eV. The edge position was defined as the onset of the intensity decrease.

For the Toluca rhabdite, the nearest distance to the edge (1.743 Å) was about 0.004 Å; for the two other specimens this distance was reduced to 0.002 Å. The following wavelengths were used: Sikhote Alin, 1.745 Å and 1.758 Å; Odessa, 1.745 Å and 1.758 Å; Toluca, 1.747 Å and 1.760 Å.

In the wavelength region 1.745–1.758 Å the value of $f'_{\rm Fe}$ varies by 2.3, whereas $f''_{\rm Fe}$ and $f'_{\rm Ni}$ change only by about 0.006 and 0.036, respectively. The number of reflections for each data set was about 730.

3. Data analysis

After the data reduction, a scaling of both sets is carried out in order to exclude some effects that interfere with the δ analysis. An iterative method (Wendschuh-Josties, 1994) was used, in which the ratio of both data sets was changed until the P atoms showed no effect in the δ map. The resulting scaling factors are 0.985 for Sikhote Alin and Odessa schreibersite and 0.91 for the Toluca rhabdite, which are reasonable values.

In the second step the measured data were combined with the corresponding phases $\varphi_{\rm C}$, calculated assuming a statistical metal distribution, to a 'mixed' structure factor $F_{\rm m}$: Sikhote Alin (Fe:Ni, 2:1), M1–M3 0.67Fe + 0.33Ni; Odessa (Fe:Ni, 1.8:1.2), M1–M3 0.6Fe + 0.4Ni; Toluca (Fe:Ni, 1.64:1.36), M1–M3 0.55Fe + 0.45Ni.

The δ density was then calculated for these three samples. Fig. 6 shows specific sections of the density distribution for the crystals from Sikhote Alin and Odessa. The density map obtained for rhabdite from the Toluca meteorite rhabdite (not shown) is similar; however, the contrast and the quality is lower. This may be a result of the larger distance of the first wavelength to the Fe absorption edge. This assumption should be verified in a further experiment.

The values of the z sections have been selected in such a way that the marked M2 atoms are placed centrally (see lower map), whereas in the upper map the section is placed above the middle of the layer between the M3 and M1 position (*cf.* Table 2). Since the position of the atoms in a layer differs only by 0.2 Å, the two maps include about half of the atoms in the unit cell.

4. Results and discussion

The results can be summarized as follows:

The δ method gives relevant results for the acentric meteoritic (Fe,Ni) phosphides.

For all measured samples, the M1 and M2 sites show an intensity in the δ map which is significantly higher than the intensity at the M3 site.

In the case of the Odessa meteorite the intensity corresponding to the M1 site seems to be somewhat higher than that for the M2 site, in contrast with the results yielded for the Sikhote Alin meteorite. For the Toluca meteorite, a difference between M1 and M2 was not observable.

The intensity corresponding to the M3 site is weak but different from zero.

Because the δ density map contains intensity arising mainly from the scattering due to Fe, it can be concluded that for all examined samples the M1 and M2 site are occupied mostly by Fe. Ni dominates at the M3 site, but some Fe could be present at this site as well. This result is also in accordance with the Fe:Ni composition of the samples.

In order to check these results, a simulation was performed using the same wavelengths as in the experiment. For the calculation of the moduli $|F_{\rm C}|$ the following model distribution was assumed: M1, Fe only; M2, 0.8Fe + 0.2Ni; M3, Ni only. The $|F_{\rm C}|$ values were then combined with the phases of a statistical metal distribution. The results of the simulation are given in Fig. 7.

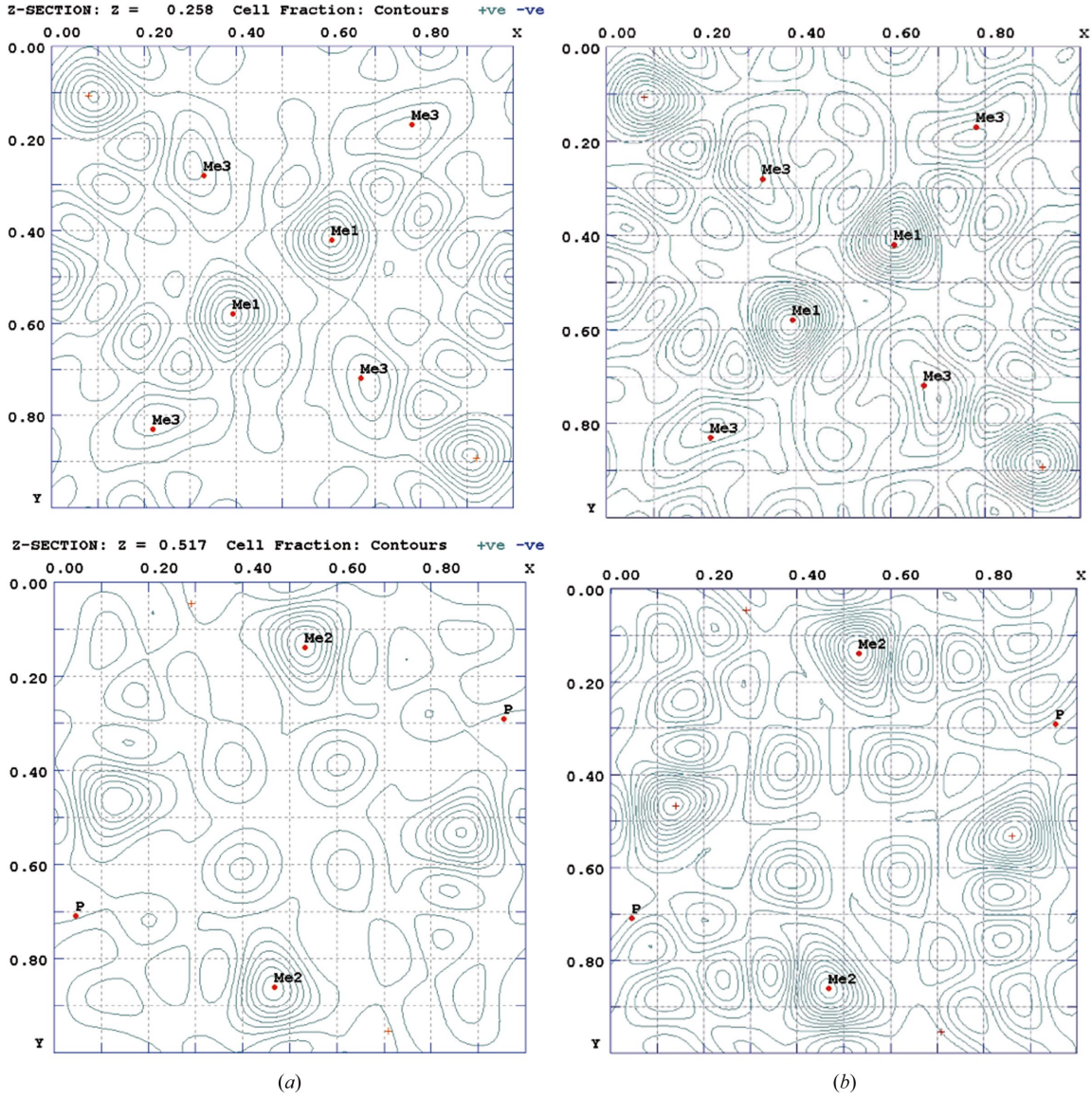

Figure 6
(*a*) δ syntheses of a schreibersite crystal from the Sikhote Alin meteorite. Data sets measured with $\lambda_1 = 1.745$ Å and $\lambda_2 = 1.758$ Å. (*b*) δ syntheses of a schreibersite crystal from the Odessa meteorite. Data sets measured with $\lambda_1 = 1.745$ Å and $\lambda_2 = 1.758$ Å.

The agreement with the experimental data (Fig. 6) is good. Also, a distinct density at the M3 site appears, although for the calculation of $|F_C|$ it was assumed that M3 is occupied by Ni only. However, a second simulation, now using phases corresponding to the ordered model, yields no remarkable density at the M3 site (Fig. 8).

Therefore it can be concluded that the information resulting from the phases, which were calculated with a statistical metal distribution, is probably responsible for the intensity at the M3 site. In contrast to other substances (*e.g.* mückeite), the method of phase approximation may not be so effective for the $(Fe,Ni)_3P$ phosphides, owing to a higher contribution of the investigated elements to the scattering power [Fe:Ni is about 84% in $(Fe,Ni)_3P$, while Cu:Ni is about 30% in $CuNiBiS_3$ (Wendschuh-Josties, 1994)]. Thus a stronger influence of the actual metal distribution on the phase angles can be expected.

Nevertheless, it was shown that the δ synthesis is also applicable for such types of structures as $(Fe,Ni)_3P$, provided that, in addition to the experiment, calculations and simulations have to be performed.

As a result of the calculations, it follows that the M3 site is probably occupied by Ni only. Furthermore, it is reasonable to assume that M1 is completely occupied by Fe. Therefore the M2 site should be then occupied by Fe and Ni, depending on the sample composition and on the M1/M2 density relation observed (Table 3).

In the δ synthesis experiment, both forms of phosphides, two chemical classes (IAB and IIAB) and Fe:Ni relations from 1.2 to 2.0, were examined, which covered a part of the meteoritic phosphides. An expansion to other chemical classes or samples with higher Ni content would be of certain interest.

A simple explanation of this metal distribution in the three structural sites M1, M2 and M3 is not known. Fe and Ni are

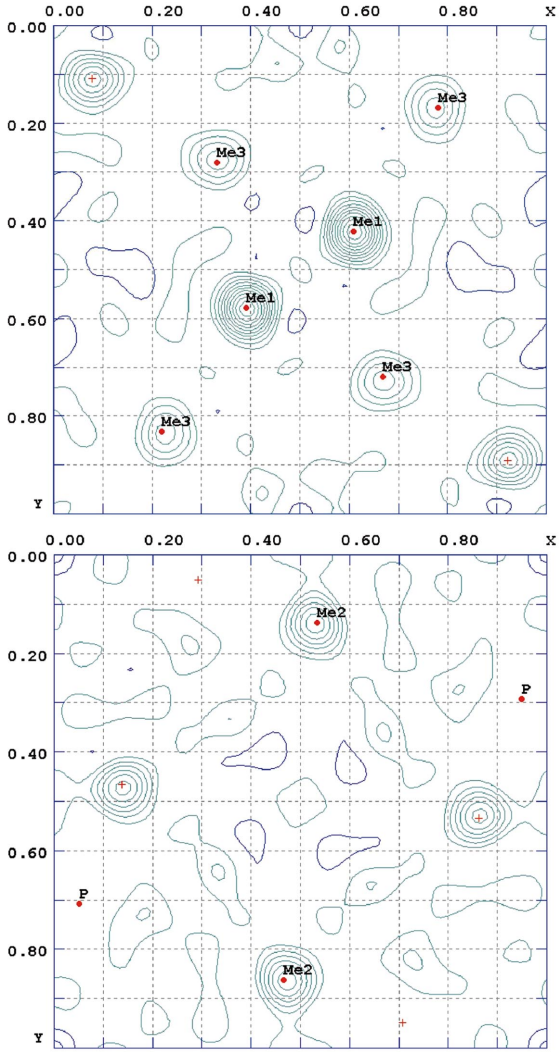

Figure 7
Simulation of the δ syntheses. $|F_C|$ is calculated for an ordered model and combined with the phases of a statistical metal distribution.

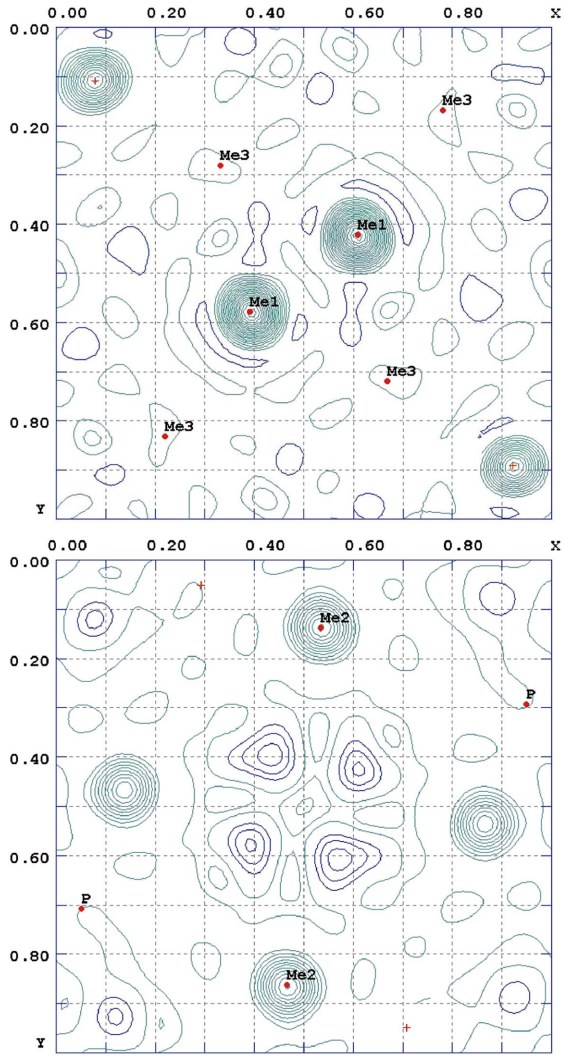

Figure 8
The same as Fig. 7 but with phases corresponding to the ordered model.

Table 3
Metal distribution obtained by the δ technique for some phosphide crystals of different iron meteorites.

CD: Canyon Diablo; SA: Sikhote Alin. The results for the Toluca and Canyon Diablo meteorite are tentative.

Phosphides (Fe:Ni)	Meteorites	M1	M2	M3	*a*/*c*
Rhabdite (1.2:1)	Toluca (IAB)	Fe	Fe, Ni	Ni	2.020
Schreibersite (1.3:1)	CD (IAB)	Fe	Fe, Ni	Ni	2.027
Schreibersite (1.5:1)	Odessa (IAB)	Fe	~0.8Fe + 0.2Ni	Ni	2.032
Schreibersite (2.0:1)	SA (IIAB)	Fe	Fe	Ni	2.031

similar elements and the coordination of the three sites provides no indices (*e.g.* Doenitz, 1970; M1 site: 2 phosphorus (P) atoms + 13 metal (M) atoms; M2 site: 4P + 10M; M3: 3P + 11M). Otherwise, comparing the obtained *a*/*c* ratio (*cf.* Table 1) and the above metal distribution, one can assume that the occupation of the M2 site with Fe is responsible for the variation of the *a*/*c* ratio.

Furthermore, for synthetic $(Fe,Co)_3P$ a similar result concerning the metal order was obtained by neutron powder diffraction experiments (Liu *et al.*, 1998): Co preferentially occupies the M3 and M2 sites, whereas Fe occupies the M1 and M2 sites but not the M3 site.

The investigation of iron-bearing schreibersite by Mossbauer spectroscopy has not yielded additional information (Ouseph *et al.*, 1979; Scorzelli & Danon, 1986). The obtained internal magnetic fields differ for the three metal positions, being smallest for the M3 site. However, this tendency was also observed for the synthetic Fe_3P. Therefore a comparison is difficult.

Thus it can be concluded that this metal distribution seems to be characteristic of this structure, independent of the thermal history, because in the case of natural meteorites the cooling rates were extremely slow (some $K/10^6$ years), contrary to synthetic materials.

This similarity between the metal ordering in meteoritic and synthetic phosphides is comparable with the correspondence

of the orientation relations found in meteoritic plessit and duplex steel (Nolze & Geist, 2004).

5. Summary

$(Fe,Ni)_3P$ crystals with crystalline quality sufficient for synchrotron studies were extracted from different iron meteorites (octahedrites).

A determination of the Fe:Ni distribution in the metal sites M1, M2 and M3 of the structure was possible using δ synthesis. The application of this two-wavelength method to crystals, where the metal atoms of interest are the dominating component in the unit cell, was possible by comparing the experimental results with simulation calculations.

For all crystals examined it was found that Ni prefers the M3 site, avoiding the M1 position. This result agrees with Doenitz (1970) and confirms results of refinements of conventional X-ray experiments. Moreover, a neutron diffraction experiment on isostructural synthetic $(Fe,Co)_3P$ yields the same trend for the distribution of Fe and Co (Liu *et al.*, 1998).

We would like to thank HASYLAB-DESY for permission to use the synchrotron facilities. This work was funded by the DFG and we are grateful for their support (Ge 497/4-1). The authors wish to thank Dr C. Hennig for his suggestions and help.

References

Aronsson, B. (1955). *Acta Chem. Scand.* **9**, 138–140.
Buchwald, V. F. (1975). *Handbook of Iron Meteorites.* Berkeley: University of California Press.
Bunge, H. J., Weiss, W., Klein, H., Wcislak, L., Garbe, U. & Schneider, J. R. (2003). *J. Appl. Cryst.* **36**, 137–140.
Clarke, R. S. Jr & Goldstein, J. I. (1978). *Smithsonian Contrib. Earth Sci.* **21**, 1–80.
Delaney, J. S. & Dyar, M. D. (2003). *Lunar Planet. Sci.* **34**, 1979.
Doan, A. S. & Goldstein, J. I. (1970). *Met. Trans.* **1**, 1759–1767.
Doenitz, F. D. (1970). *Z. Kristallogr.* **131**, 222–236.
Geist, V., Wagner, G., Nolze, G. & Moretzki, O. (2005). *Cryst. Res. Techn.* **40**, 52–64.
Jochum, K. P., Seufert, M. F. & Begemann, F. (1980). *Z. Naturforsch. Teil A*, **35**, 57–63.
Jörchel, P., Szymanski, A., Hennig, C. & Geist, V. (2000). DGK-Tagung 2000, Aachen, p. 169.
Liu, H. P., James, P., Broddefalk, A., Andersson, Y., Graneberg, P. & Eriksson, O. (1998). *J. Magn. Magn. Mater.* **189**, 69–82.
Moretzki, O. (1999). Thesis, University Leipzig, Germany.
Moretzki, O., Doering, Th., Geist, V., Morgenroth, W. & Wendschuh, M. (2003). *Z. Kristallogr.* **218**, 391–396.
Nolze, G. & Geist, V. (2004). *Cryst. Res. Technol.* **39**, 343–352.
Ouseph, P. J., Groskreutz, H. E. & Johnson, A. A. (1979). *Meteoritics*, **14**, 97–108.
Reed, S. J. B. (1965). *Geochim. Cosmochim. Acta*, **29**, 513–534.
Rundquist, S. (1962). *Acta Chem. Scand.* **16**, 1–19.
Scorzelli, R. B. & Danon, J. (1986). *Meteoritics*, **21**, 509.
Skála, R. & Císařová, I. (2001*a*). *Lunar Planet. Sci.* **32**, 1564.
Skála, R. & Císařová, I. (2001*b*). *Meteorit. Planet. Sci. (Suppl.)* **36**, A191.
Skála, R. & Drábek, M. (2003). *Mineral. Mag.* **67**, 783–792.
Sutton, S. R., Delaney, J. S., Smith, J. V. & Prinz, M. (1987). *Geochim. Cosmochim. Acta*, **51**, 2653–2662.
Tagai, T., Takeda, H. & Fukuda, T. (1992). *Meteoritics*, **27**, 295.
Wendschuh-Josties, M. (1990). Thesis, University Göttingen, Germany.
Wendschuh-Josties, M. (1994) *Z. Kristallogr.* **209**, 107–112.
Wulf, R. (1990). *Acta Cryst.* A**46**, 681–688.